A novel experimental set-up for *in-situ* microstructural characterization during continuous strain path change

IOP Conf. Series: Materials Science and Engineering **967** (2020) 012007 doi:10.1088/1757-899X/967/1/012007

A novel experimental set-up for *in-situ* microstructural characterization during continuous strain path change

S Dhara[1]*, S Taylor[1], Ł Figiel[1], B Shollock[2] and S Hazra[1]

[1] *WMG, University of Warwick, Coventry, CV4 7AL, UK*

[2] *Department of Engineering, King's College London, London, WC2R 2LS, UK*

* *Email: Sisir.Dhara@warwick.ac.uk*

Abstract

Strain path change is a typical phenomenon during continuous stamping operations of sheet metal for a variety of applications including automotive body parts. During stamping, a punch continuously deforms a metal sheet to produce a desired geometry while following various strain path transitions depending on overall design of the stamping process. The strain path change can potentially alter the expected forming limit of the material. Previous researchers investigated the effect of changing strain path by loading sample in two distinct steps. Typically, between the steps the sample is unloaded before being re-loaded in the new strain path. This practice reflects the key challenge in elucidating this strain path dependent deformation, which is the ability to control the strain path change in a single deformation stage in an experimental set-up. In this work, a novel testing rig and specimen geometry that is capable of changing the strain path of a sample continuously without unloading the specimen were conceptualised, modelled and subsequently manufactured. Using this apparatus, the specimen was deformed in the uniaxial strain path in the first step before being deformed biaxially without unloading in between the steps. Thus, the apparatus ensures that the sample undergoes a continuous strain path change without unloading between the steps. The size of this mechanical test rig permits it to be placed inside a scanning electron microscope (SEM) chamber in order to study strain path transition *in-situ* to highlight strain localization and related microstructural changes in real time. Utilizing this test set-up, strain path change and corresponding strain values along each strain path were evaluated. The changes in material microstructure were concurrently investigated using *in-situ* SEM and electron back scattered diffraction (EBSD) analysis.

Keywords: Strain Path Change, Finite Element Modelling, Microstructural Characterization, *In-situ* SEM and EBSD.

Corresponding author

Sisir Dhara

WMG, University of Warwick

Coventry, CV4 7AL, UK

Email: Sisir.Dhara@warwick.ac.uk

1 Introduction

The automotive sector and its suppliers are one of the largest manufacturers of stamped components. Stamping is a multi-stage process where a sheet material is drawn in the first stage and then redrawn, flanged and pierced in subsequent stages. It is common for the material to undergo two types of strain path change: a continuous strain path change in the draw stage and a discontinuous strain path change when the drawn shell is re-drawn and flanged in subsequent stages. In the first mechanism, the strain path change occurs when material is drawn and stretched over a typically complex tool geometry. In the second mechanism, the strain path change occurs when the pre-strained drawn shell is unloaded from the draw tools and subsequently re-drawn or flanged along a different strain path. The effect of strain path changes have been shown by Graf and Hosford [1], [2]. Their experiments replicated the discontinuous mechanism of strain path change. They studied the effect of uniaxial, biaxial and plain strain pre-strain on the forming limit of Al 2008 T4 aluminium alloy. It was found that the biaxial pre-strain lowered the forming limits. However, the pre-straining in uniaxial tension raised the forming limits when the direction of pre-strain was normal to rolling direction. The pre-straining near plane strain produced a slight increase in forming limits when the direction of pre-strain was normal to rolling direction. Dhara et al. [3] expanded on this work by using a Zwick tensile machine to pre-strain AA 5754-O aluminium alloy in uniaxial tension and then re-loaded their samples in the biaxial strain path using a Nakajima test with a 50 mm diameter punch. They found that the forming limit strains of the pre-strained materials were increased when the pre-strain direction was along transverse direction. However, the limiting strains decreased when the rolling direction was the pre-strain direction. Collins et al. [4] uniaxially pre-strained low carbon ferritic steel samples in a stamping press and then re-loaded their samples in the biaxial strain path using a purpose-built biaxial tester. They found that a uniaxial pre-strain followed by biaxial deformation provided a significant gain in strain to failure. A common characteristic of these experiments into discontinuous strain path change is that the two stages were carried out on different experimental setups and the samples may have experienced dis-similar loading strain rates during both stages.

The effect of changing strain path on formability is thought to be due to the way it changes the texture and work hardening of the material. To investigate the relationship between external loads and microstructure, Ghadbeigi et al. [5] and Celotto et al. [6] used a recently developed experimental technique where mechanical tests were carried out in the chamber of an SEM using a miniaturised test rig with the aim of imaging the deformation of the sample *in-situ*. They proportionally loaded their samples in the uniaxial strain path using a test rig that was compact enough to fit in the chamber of a scanning electron microscope (SEM). They imaged their samples periodically during the test and post-processed using the digital image correlation (DIC) technique to analyse the full-field strain of the samples at the meso-scale. At this scale, they were able to analyse the effect of the external loading on the strain distribution in the ferritic and martensitic phases of their dual-phase 1000 (DP1000) steel and transformation induced plasticity 800 (TRIP800) steel materials respectively. Subsequently, they observed the micro-void nucleation and fracture mechanism. Caër and Pesci [7] contributed to the design of sample for the *in-situ* deformation technique. The designed sample ensured the strain localisation at the centre of the sample and using the sample in a micromechanical test rig, they examined grain rotation and misorientation development in an annealed AISI 304 stainless steel *in-situ* during biaxial loading. Similarly to Ghadbeigi et al. and Celotto et al., they placed their test rig in an SEM to measure the evolution of texture by measuring electron back scattered diffraction (EBSD) data *in-situ* from the centre of the biaxial specimen periodically during the loading process. They explained that the loading path had a potential to orient the grains along a particular direction. Kubo et al. [8] carried out a biaxial tensile test of interstitial free (IF) steel using a biaxial specimen with the notch at the four corners of the central part in an SEM chamber and studied inverse pole figure (IPF) maps, grain average misorientation (GAM) maps and Taylor factor (TF) maps to characterise microstructural changes during biaxial tension. Conclude that this *in-situ*

technique can be used to measure the evolution of strain and texture during plastic deformation and that it is a useful tool in understanding the formability of material that undergo strain path changes. The gap is the lack of a method to change strain path during a mechanical test.

The aim of this work is to develop an experimental method to investigate the effect of the continuous strain path transition that occurs in the drawing stage on material microstructure. A Micromecha biaxial testing rig was used with a cruciform sample design based on the Caër and Pesci's design. The design was modified to enable the strain path change to occur at a set point during the experiment. The strain evolution of the samples were observed at the macroscopic and microscopic scales using DIC while the texture evolution was observed with EBSD. Initial results showed that the modified sample design was effective at altering the applied strain path and that the material experienced observable changes to its strain path and texture.

2 Development of the methodology for continuous strain path change

A Micromecha Proxima test rig was used for the strain path transition experiment. The test method was developed in two steps. In the first step, the strain evolution of a cruciform sample was analysed along a proportionate biaxial load path. In the second step, the cruciform sample was redesigned to allow a change in the strain path during loading.

The rig and the specimen used in the first step is presented in Figure 1. The horizontal (inline grips) and vertical (transverse grips) grips of the rig are connected through a 45° wedge (Figure 2b). A motor drives one end of the horizontal grip while the other end is securely fastened to the body of the rig. When the motor moves the horizontal grips, its motion is translated into a vertical motion via the wedge, thus loading the sample vertically at the same time. The inline grip was moved along X-axis and the transverse grips were moved along Y-axis during the experiments. The external dimension of the cruciform sample was 30 mm by 30 mm and its thickness was 1.2 mm (Figure 2a). The central region was reduced in thickness (0.25 mm) to concentrate the strain in that region and to prevent overloading the rig and the load cell. DP600 steel was chosen for the specimen material, as it is a high strength material used commonly in automotive applications. The material properties and chemical compositions are detailed in Table 1 and Table 2 respectively. The rig and sample were modelled using the finite element (FE) method. The validated model was used as the basis for the second step. The model consisted of the horizontal grips, vertical grips and the sample (Figure 2b). The grips and the gripping areas of the sample were modelled as rigid bodies while the sample was modelled as a deformable body. All bodies were meshed with solid elements of an appropriate size that optimised speed and accuracy. Yielding was modelled with the von Mises model and power-law hardening was assumed. The yield model and hardening law were chosen the simplest one as the finite element modelling was done to optimize the design of sample and overall assembly. The anisotropy coefficient of the sample material was nearly 1 and hence, isotropic material model was considered to simplify the model. More advanced material model such as crystal plasticity based model with anisotropic behaviour and hardening law were beyond the scope of current research and would be studied in future. To model the clamping of the sample to the grips, the nodes in the sample gripping areas were joined to the nodes of the grips as constrained rigid bodies. Displacement (1.5 mm) was applied to in-line grip 1 along X-axis (Figure 2b) to represent the motor in the physical rig. Inline grip 2 was fixed. The motion of transverse grips 1 and 2 was restricted to the Y-axis, to reflect the physical rig. The model was solved using LS-Dyna explicit v.10.1.0. The X-axis (ε_x) and Y-axis (ε_y) strain contour shows the strain concentration and uniformity of the strain distribution at the central region (Figure 3a-b). The strain path at the centre of the specimen showed that the specimen was undergone biaxial strain path (Figure 3c).

The model was validated against physical trials. During trial experiments with the rig and the biaxial sample, the strain evolution at the centre of the specimen needs to be calculated in order to confirm

whether the specimen is suitable enough for performing biaxial elongation and suitable for *in-situ* experiment. The strain evolution of the sample during the experiment was measured with the GOM 12M macro-DIC system. The DIC system consisted of two 12MP cameras fitted with lenses to capture the strains in the arms and central region of the specimens. Measurement frame rate was 1 frame/second and samples were loaded at 0.3 mm/min. The experimental ε_x and ε_y strain contour of the specimen is presented in Figure 4a-b. The strain path at the centre of the specimen was analysed from the experiment and depicted in Figure 4c. There was some slack at the start of the experiment as the loading mechanism fully loaded the specimen. After ε_x=0.02, the strain path was similar to that predicted by the FE model (slope of 1.2 experimental vs 1.1 predicted).

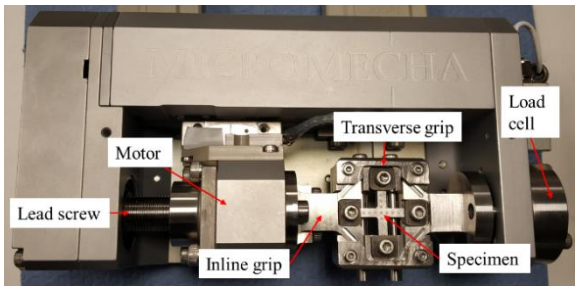

Figure 1: Experimental set-up consisting of the rig and the specimen

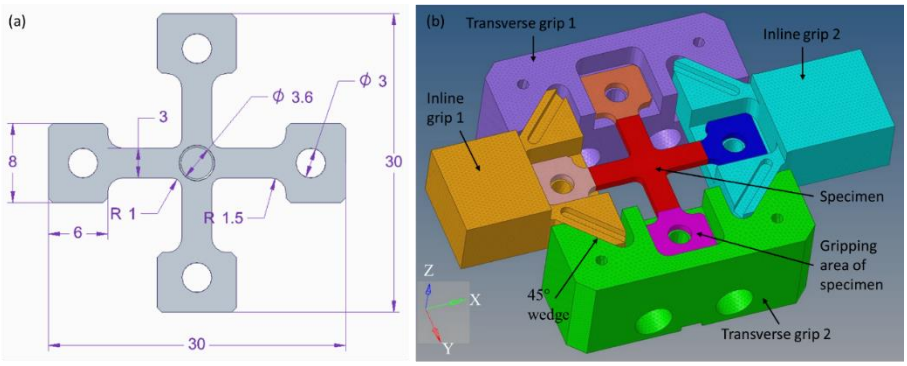

Figure 2: (a) Biaxial stretching specimen and (b) FE model of the assembly consists of the rig and the specimen

Table 1: Material properties of DP600 steel used in this work

Material		DP600
Gauge (mm)		1.2
Young modulus (GPa)		208
Yield strength (MPa)		407
Ultimate tensile strength (MPa)		665
% Elongation		22
Anisotropy parameters	r_0	0.96
	r_{45}	0.93
	r_{90}	1.05
Hardening parameters according to Hollomon law	Strength coefficient, K (MPa)	1125
	Hardening exponent, n	0.21
Density (g/cm^3)		7.87
Poisson's ratio		0.3

Table 2: Chemical composition (wt %) of DP600 steel used in this work

Material	C	Mn	Si	Al	Mo	Cr	Cu	S	P	Fe
DP600	0.09	1.84	0.36	0.05	0.01	0.02	0.03	0.005	0.01	Balance

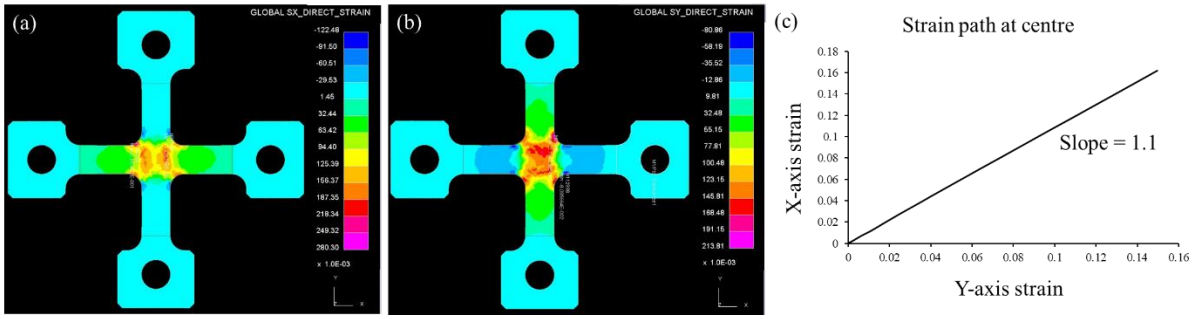

Figure 3: (a) X-axis and (b) Y-axis strain contours of the specimen predicted from FE modelling, and (c) predicted strain path at the centre of the specimen during biaxial stretching

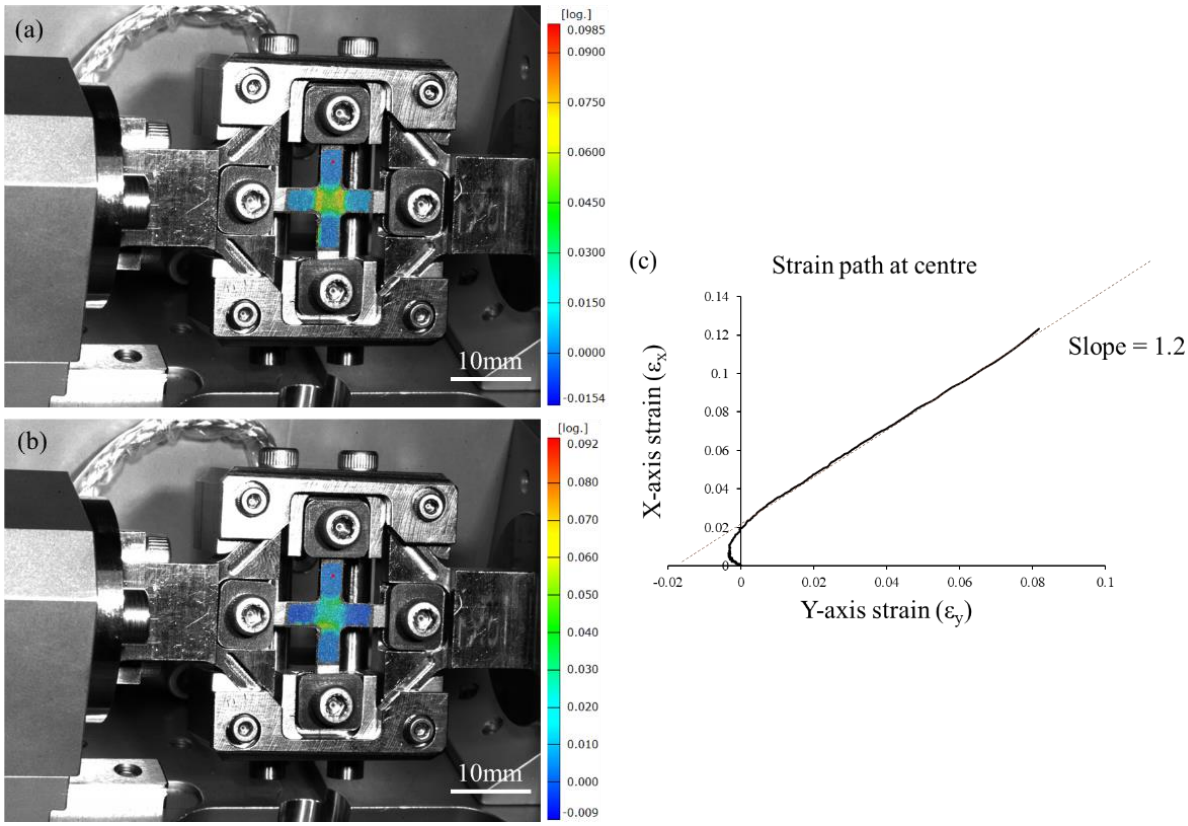

Figure 4: Experimental strain contour: (a) X-axis and (b) Y-axis strain contour superimposed on the specimen, and (c) strain path at the centre of the specimen during biaxial stretching

To change the strain path during testing, the cruciform specimen geometry was modified to include slotted holes in the vertical arms (Figure 5a). At the start of the test, the slots allowed the bolts of the vertical (transverse) grips to translate without loading the sample. After a specified elongation that is determined by the length of the slots (0.2 mm), the transverse grips engage and the specimen is deformed biaxially. Hence, the material is deformed uniaxially at the start of the test before the strain path changes to biaxial strain path. The test in step 1 was repeated with this modified sample geometry. It ensured that the specimen was loosely held in the transverse grips to allow the grips to travel freely in the 0.2 mm slot in the first stage of the travel (Figure 5b). The experimental ε_x and ε_y contour of the specimen before and after the strain path transition was evaluated and is presented in Figure 6a-d. The ε_x and ε_y strain evolution at the centre of the specimen showed that the sample was deformed uniaxially initially and then biaxially towards the end of the test (Figure 6e).

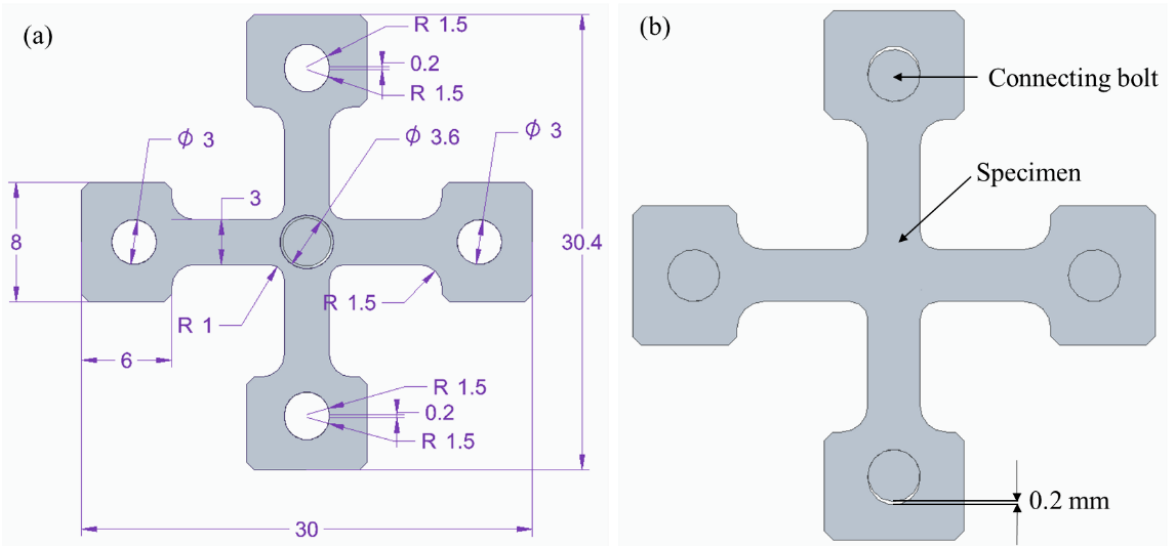

Figure 5: (a) Design of strain path change specimen and (b) assembly design showing 0.2 mm travel of connecting bolt during strain path change

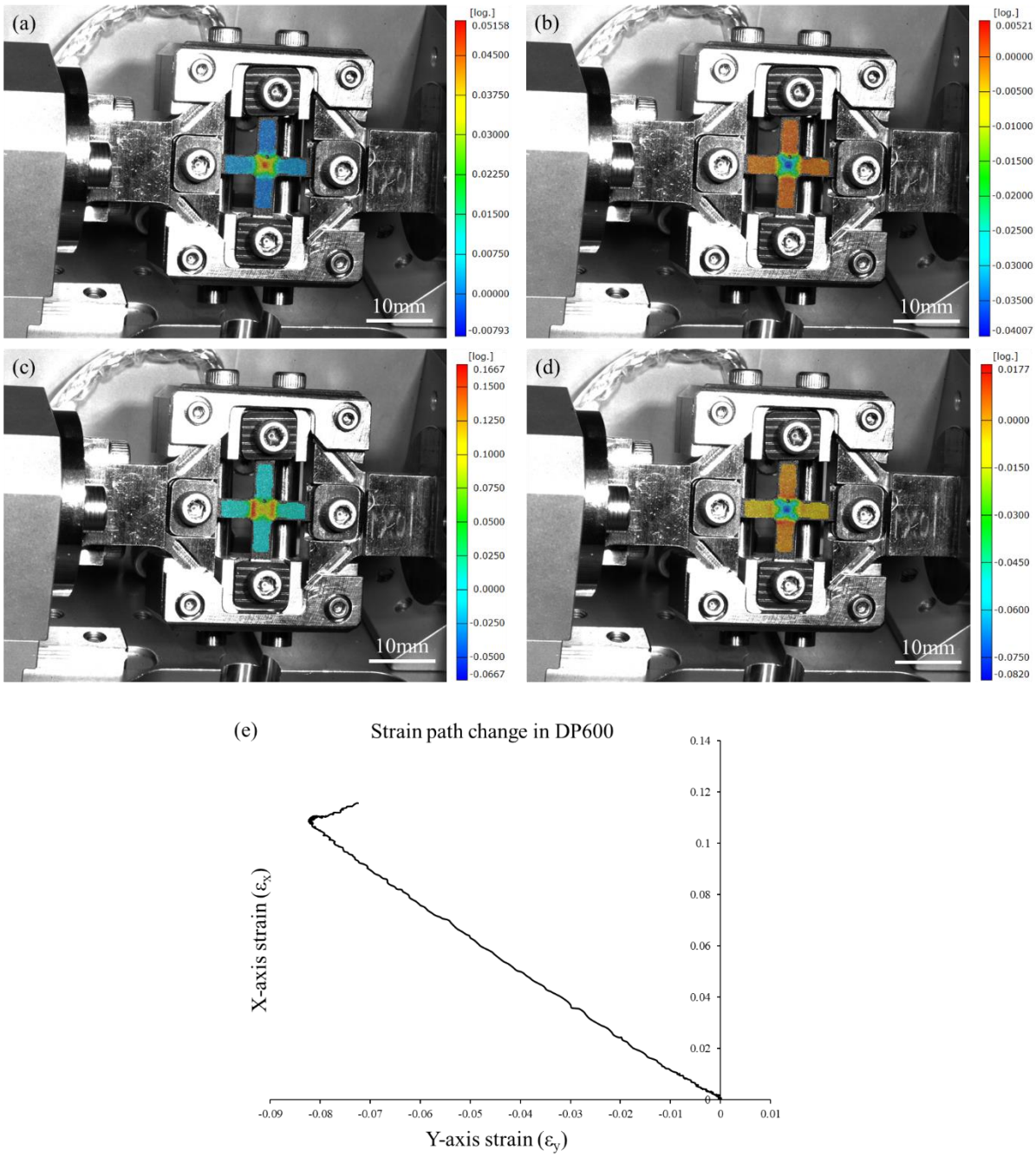

Figure 6: Experimental strain contour: (a) X-axis and (b) Y-axis strain contour superimposed on the specimen before strain path transition, (c) X-axis and (d) Y-axis strain contour superimposed on the specimen after strain path transition, and (e) strain path change at the centre of the specimen

3 Measuring microstructural strains and texture evolution during continuous strain path change

The specimens for strain path change were prepared from DP600 steel sheet and were polished by using silicon carbide (SiC) paper, diamond suspension solutions and finally 0.05 µm colloidal silica solution. Samples for microstructural strain evaluation were etched with 2% Nital solution for 10 seconds. The etched sample was loaded in the rig. To carry out the microstructural measurements, the rig was placed

in the chamber of a ZEISS SIGMA field emission gun scanning electron microscope (FEG-SEM). The rig was controlled using the POROS 2 software supplied with the Micromecha rig. The inline grip was elongated at a rate of 5 µm/sec. The elongation was arrested every 0.2 mm travel to perform SEM and EBSD scans for strain and texture analysis respectively. The microstructural observations consisted of micro (grain level) DIC analysis and EBSD analysis. For micro DIC analysis, the SEM scan was done by using secondary electrons (SE2) with 20 keV voltage. The captured SEM images were post-processed with Lavision's digital image correlation software (Davis 10) to obtain the distribution of strain in the microstructure. The subset size was used as 25 µm and step size was used as 8 µm during the analysis. The test was repeated to obtain texture measurements with the SEM's EBSD detector. During EBSD scanning, the step size was kept at 0.5 µm. The EBSD results were analysed in HKL Channel 5 software. These *in-situ* measurements allowed the detailed analysis of microstructural deformation as a result of the continuous strain path change.

4 Results and discussion

The ε_x and ε_y strain distributions calculated from micro DIC analysis show that the strain distributions are heterogeneous with a wide spread of strains (Figure 7 and 8). This is because the dual phase steel is made up of a hard martensite phase and a softer ferrite phase. Lower strains are approximately associated with the martensite phase. During the initial stage of the experiment when the sample was loaded uniaxially, ε_x increased while ε_y decreased. Based on the average strains in the data, the $\varepsilon_y/\varepsilon_x$ ratio was found to be -0.75, which is in between uniaxial tension (ratio -0.5) and pure shear deformation (ratio -1.0). This may be due to the extent of the strain variance as a result of the heterogeneity of the microstructural strain field. After 1 mm elongation of inline grip, the ε_y started to increase confirming that the strain path change (uniaxial to biaxial) started after 1 mm elongation of the inline grip. The banding of ε_x and ε_y strain (indicated by black line in Figure 7 and 8) align approximately 45° to the initial loading direction. When the strain path change occurs, the angle of these lines appears to rotate. The rotation is more prominent in ε_x strain distribution than ε_y strain distribution. Further analysis on microstructural changes was performed by carrying out EBSD mapping of around 250 grains at the centre of the specimen. The EBSD maps are shown in Figure 9 along with the inverse pole figure (IPF) Z colouring. Evidence of deformation was clear within the grain structure, with grain elongation and rotation occurring with increased elongation of the sample. During the strain path change, some of the grains (indicated by black dotted circle in Figure 9) underwent rotation and their crystallographic direction changed from [101] towards [001]. The grain rotation was further studied with the help of pole figures as shown in Figure 10. There was a difference in colour contour in the pole figures in {100} and {111} plane before and after the strain path transition with a noticeable increase in multiples of uniform distribution (MUD) values immediately before failure.

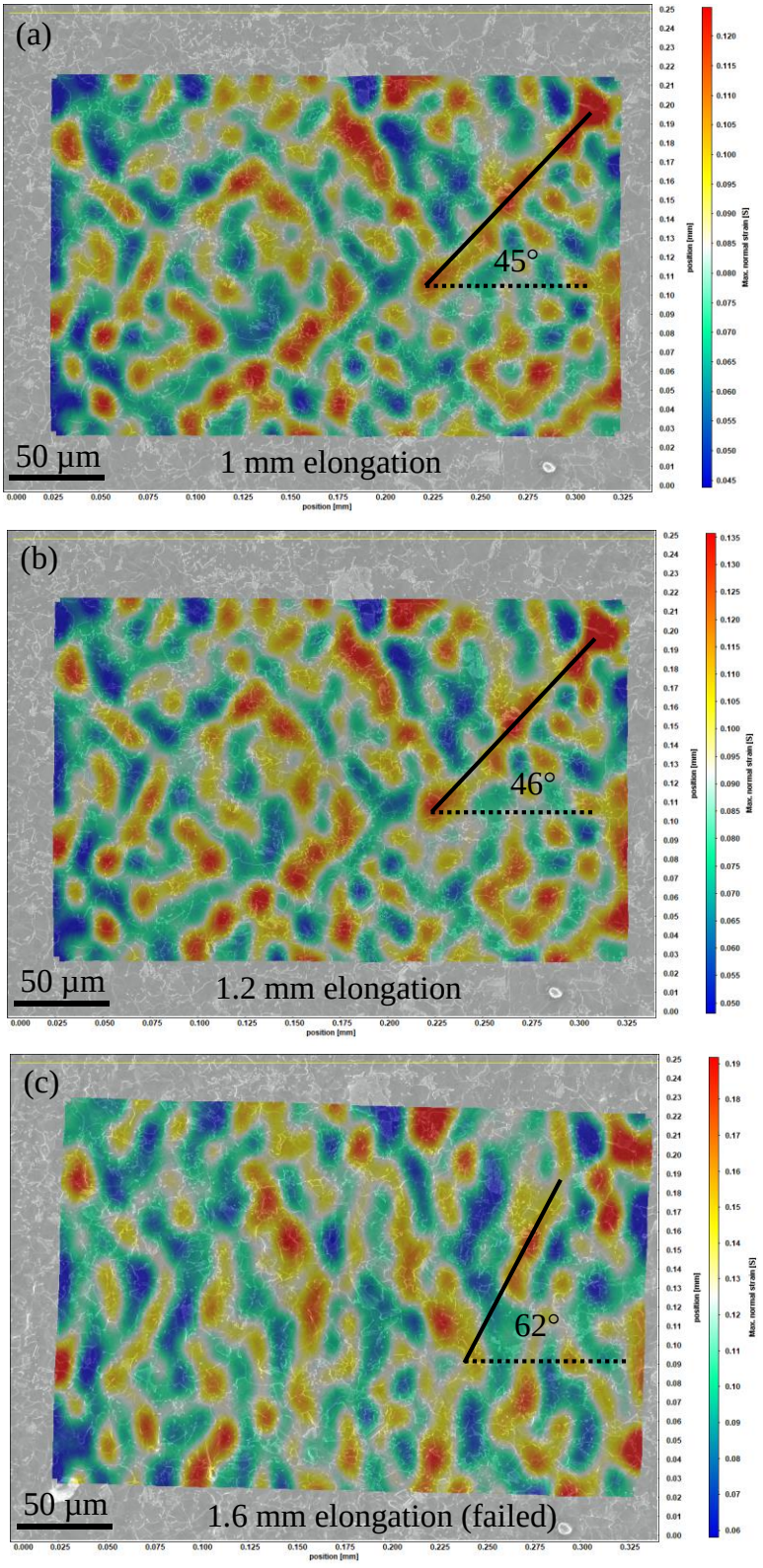

Figure 7: ε_x strain distribution at the centre of the specimen calculated from micro DIC analysis after (a) 1 mm, (b) 1.2 mm and (c) 1.6 mm elongation of the specimen along X-axis during strain path change

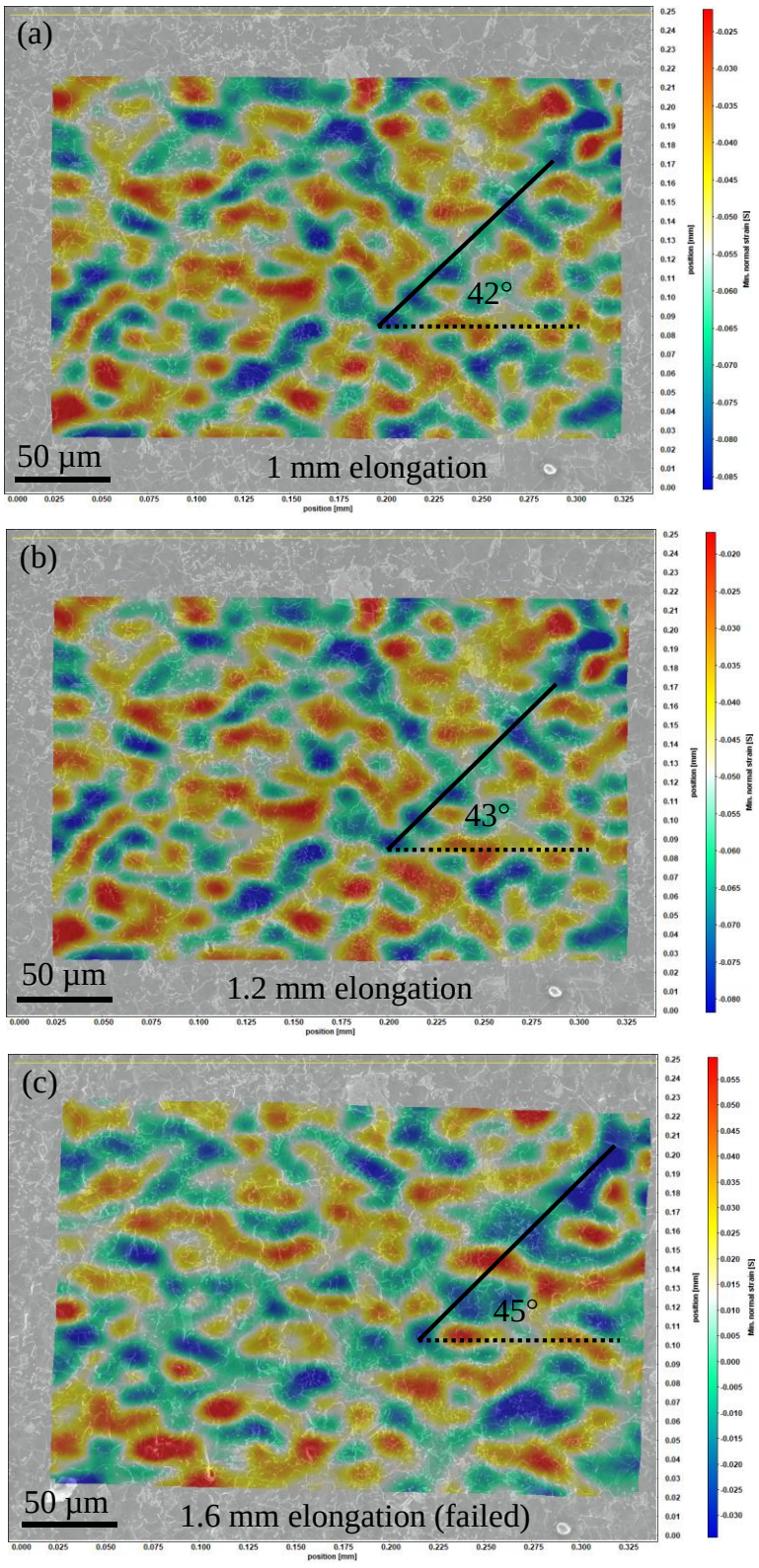

Figure 8: ε_y strain distribution at the centre of the specimen calculated from micro DIC analysis after (a) 1 mm, (b) 1.2 mm and (c) 1.6 mm elongation of the specimen along X-axis during strain path change

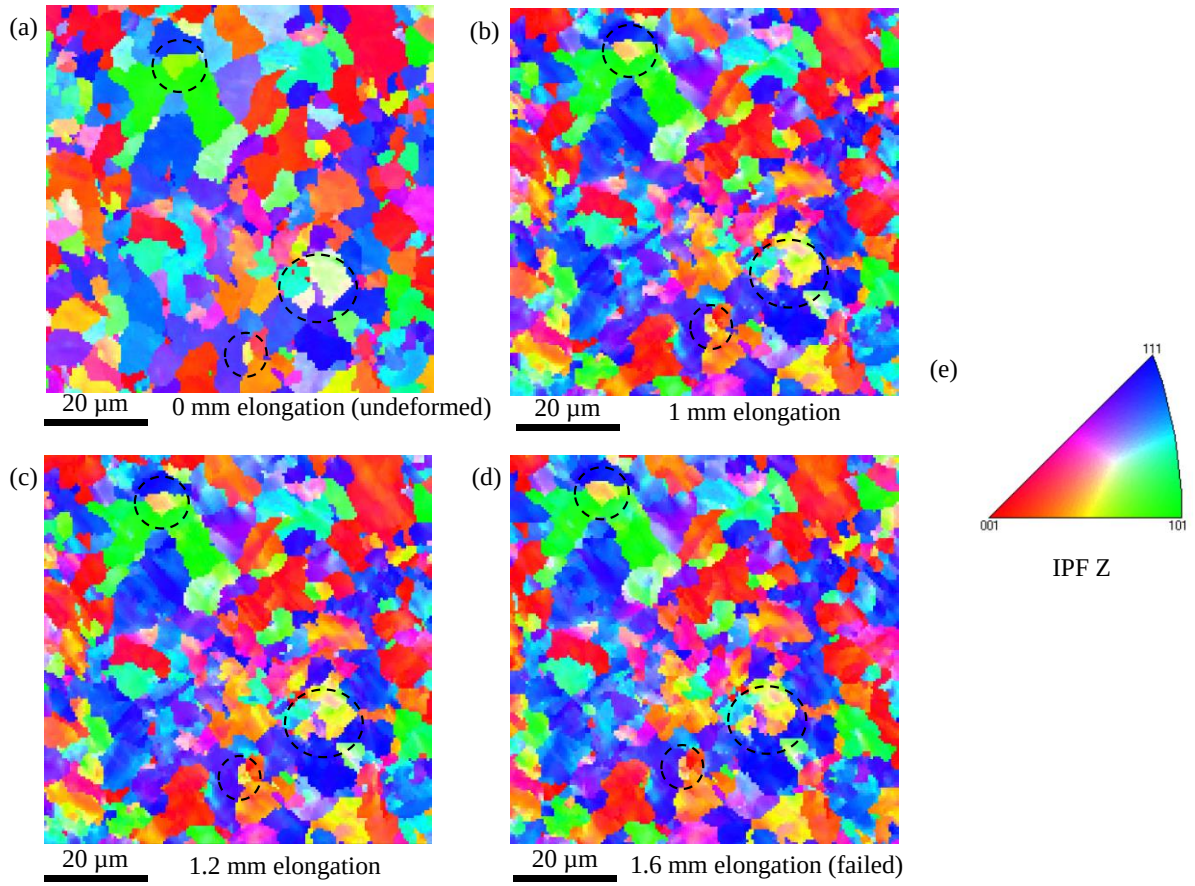

Figure 9: EBSD mapping of the grains at the centre of the specimen after (a) 0 mm, (b) 1 mm, (c) 1.2 mm and (d) 1.6 mm elongation of the specimen along X-axis during strain path change, and (e) IPF Z colouring

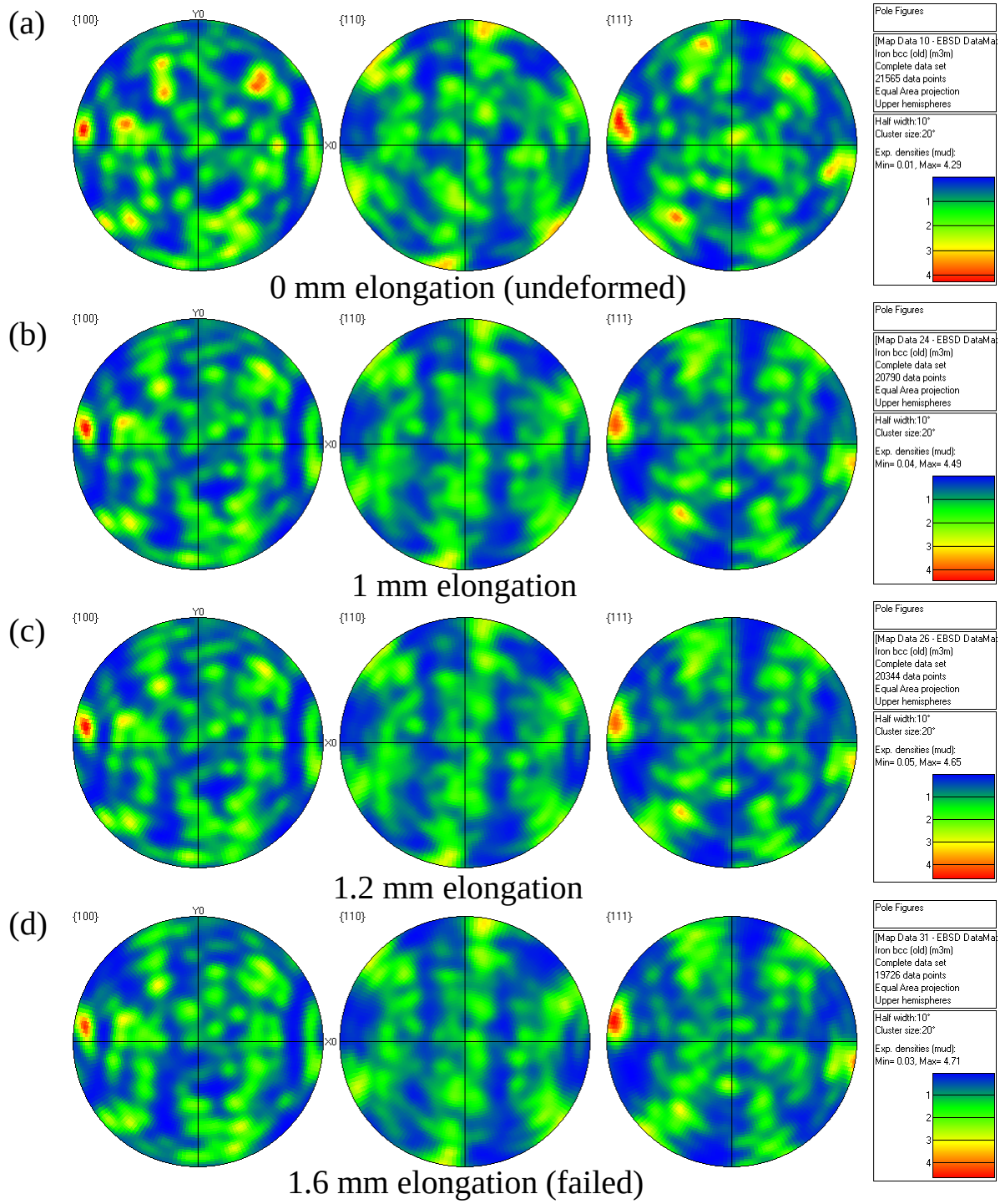

Figure 10: Pole figures of the grains at the centre of the specimen after (a) 0 mm, (b) 1 mm, (c) 1.2 mm and (d) 1.6 mm elongation of the specimen along X-axis during strain path change

5 Conclusions

An experimental technique was developed to test cruciform samples along (a) a proportional strain path and (b) a non-proportional strain path. Suitable specimen for proportional and non-proportional strain

path change was also designed. The mechanism developed for strain path change has the potential to perform strain path transition continuously without withdrawal of the applied load from the specimen. DIC analysis at macroscale showed that the DP600 steel specimen underwent biaxial strain path in proportionate test and uniaxial to biaxial strain path transition in the non-proportionate test. Hence, the mechanism is ideal to study the effect of strain path change. Moreover, as the overall set-up can easily be placed inside an SEM chamber, performing microstructural analysis was extremely simple during strain path change. DIC analysis at microscale revealed the heterogeneous strain banding on the sample surface and the angle of the bands was rotated as the strain path transition occurred. The EBSD and pole figure results confirmed the evidence of grain rotation during strain path change. Thus, DP600 steel is susceptible to grain rotation during strain path transition. The microscale DIC and EBSD analysis confirmed that the microstructural evolution could easily be tracked during *in-situ* strain path change using the developed mechanism. In future, a detailed study on the microstructural changes will be carried out during strain path change.

References

[1] A. F. Graf and W. F. Hosford, "Calculations of forming limit," *Metall. Trans. A*, vol. 24, no. 11, pp. 2497–2501, 1993.

[2] A. Graf and W. Hosford, "The influence of strain-path changes on forming limit diagrams of A1 6111 T4," *Int. J. Mech. Sci.*, vol. 36, no. 10, pp. 897–910, 1994.

[3] S. Dhara, S. Basak, S. K. Panda, S. Hazra, B. Shollock, and R. Dashwood, "Formability analysis of pre-strained AA5754-O sheet metal using Yld96 plasticity theory: Role of amount and direction of uni-axial pre-strain," *J. Manuf. Process.*, vol. 24, pp. 270–282, 2016.

[4] D. M. Collins *et al.*, "A synchrotron X-ray diffraction study of non-proportional strain-path effects," *Acta Mater.*, vol. 124, pp. 290–304, 2017.

[5] H. Ghadbeigi, C. Pinna, S. Celotto, and J. R. Yates, "Local plastic strain evolution in a high strength dual-phase steel," *Mater. Sci. Eng. A*, vol. 527, no. 18, pp. 5026–5032, 2010.

[6] S. Celotto, H. Ghadbeigi, C. Pinna, B. A. Shollock, and P. Efthymiadis, "Deformation-Induced Microstructural Banding in TRIP Steels," *Metall. Mater. Trans. A*, vol. 49, no. 7, pp. 2893–2906, 2018.

[7] C. Caër and R. Pesci, "Local behavior of an AISI 304 stainless steel submitted to in situ biaxial loading in SEM," *Mater. Sci. Eng. A*, vol. 690, pp. 44–51, 2017.

[8] M. Kubo *et al.*, "Development of Biaxial Tensile Test System for *In-situ* Scanning Electron Microscope and Electron Backscatter Diffraction Analysis," *ISIJ Int.*, vol. 56, no. 4, pp. 669–677, 2016.